

A Bar/Bulge model for the Milky Way

Inma Martinez-Valpuesta¹

¹ Max-Planck-Institut für Extraterrestrische Physik, Giessenbachstrae, D-85748 Garching, Germany

Abstract

Bars are strong drivers of secular evolution in disk galaxies. Bars themselves can evolve secularly through angular momentum transport, producing different boxy/peanut and X-shaped bulges. Our Milky Way is an example of a barred galaxy with a boxy bulge. We present a self-consistent N-body simulation of a barred galaxy which matches remarkably well the structure of the inner Milky Way deduced from star counts. In particular, features taken as signatures of a second “long bar” can be explained by the interaction between the bar and the spiral arms of the galaxy. Furthermore the structural change in the bulge inside $l = 4^\circ$ measured recently from VVV data can be explained by the high-density near-axisymmetric part of the inner boxy bulge. We also compare this model with kinematic data from recent spectroscopic surveys and estimate the pattern speed of the bar of the Milky Way.

1 Introduction

For many years the Milky Way has been considered a barred galaxy [14]. But barred galaxies do not come of just one type, and different properties of the bar affect the dynamics in a great variety of ways: spiral arms location, resonances, gas inflow, and many more ways. In the last two decades the bar length, orientation angle and pattern speed have been highly debated.

The Milky Way (MW) is considered to have a boxy bulge, also sometimes called the triaxial bulge, as clearly revealed by infrared observations from the COBE/Diffuse Infrared Background Experiment [44]. The boxy bulges are associated to bars through buckling instability and secular evolution [12, 11, 33], and observationally studied by [29] and [7]. The boxy bulge in the MW has been identified and studied with star counts [41, 40, 42, 24] giving constraints on the triaxiality of the bulge. Also the study of the asymmetries in the COBE data [16, 5] led to the first dynamical models of the MW.

In the last decade new star counts and infrared data have confirmed the existence of an extra component at higher longitudes of $l \sim 28^\circ$ [21, 4, 9, 25, 8] indicating a longer and flatter structure. This long and flat structure has been lately interpreted as the flatter parts of an evolved bar after the buckling instability, unifying the boxy bulge bar and the long and flat structure with a quantitative study by [27] and also qualitatively described in [2, 38].

The formation and evolution of the MW has been revisited lately when new simulations have been compared with kinematical data. [39] compared a self consistent model with rigid halo with the BRAVA kinematical data where no more than 8% of bulge mass was needed to fit the data. Also very recently, [30] presented metallicity observational data where they interpreted their results without the need of a classical bulge. These results could imply that the MW is in contradiction with the actual cosmological standard scenario where most galaxies would necessarily have a classical bulge. Therefore the MW evolution could be one of the biggest challenges within the actual understanding of evolution of galaxies.

In the last decade, to understand the MW structure and its possible formation a new approach has been attempted by means of dynamical models [6, 35]. In these two works, the bar has been considered as one short boxy bulge, ignoring the long and flat part. In the former they match quite well the proper motions in the Baade's window. The predictions of proper motions in the latter were in rough agreement with the observed data by [43], and they also appeared to be more anisotropic.

In this work we will describe how a secularly evolving bar can reproduce the star count data for different regions of the bar and the kinematical observational data.

2 A MW like N-Body model

The simulation we used in [27] is similar to that published in [26] and was not run to match the MW structure. The code used was FTM 4.4 (updated version) from [22]. The total number of particles is 1×10^6 , distributed initially in an exponential disk with $Q = 1.5$, embedded in a live dark matter halo. After ~ 1.5 Gyr the bar becomes very strong and buckles, thereby weakening. Later the bar resumes its evolution and grows again, resulting in a prominent *boxy bulge and bar* structure.

Fig. 1 shows the simulated galaxy at time ~ 1.9 Gyr, after the boxy bulge has formed and the bar has regrown. The face-on density distribution for this snapshot is shown in Figure 1 (upper panel), oriented at an angle $\alpha = 25^\circ$ with respect to the line from the Galactic centre to the observer. The boxy bulge is apparent in Fig. 1 (lower panel). The Sun was placed at 8 kpc. The model was scaled so that the end of the planar bar appears just inside longitude $l = 30^\circ$ as seen from the observer. The bar length is ~ 4.5 kpc, and the maximum ellipticity is 0.46.

In the face-on view can be clearly seen the *curved, leading* ends of the stellar bar. Over time, the model shows oscillations from leading through straight to trailing ends and back. Similar morphology can be seen in other barred simulations in the literature (e.g. model m08 [17]; model B2.25 [36]) and also in some galaxies such as NGC 3124 and NGC 3450. The oscillations between trailing and leading ends of the bar could be related to the oscillations

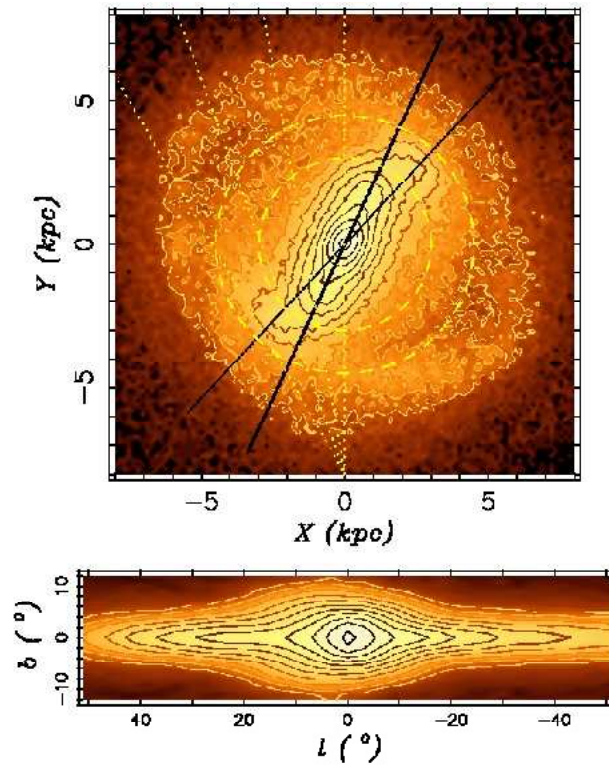


Figure 1: *Upper panel:* Face-on view of the simulation at time $T \sim 1.9$ Gyr. The bar rotates clockwise. The model has been scaled to the MW and is oriented such that the long axis of the bulge is seen at an angle $\alpha = 25^\circ$ by the observer at $(0, -8$ kpc). A second line at 43° as inferred for the *long-bar* in the MW is also shown. *Lower panel:* edge-on view of the same snapshot, as viewed from the Sun. The boxy structure is noticeable. Higher densities correspond to brighter colours (as in [27])

seen in the bar growth in N-body simulations (e.g. [15]) and may be due to non-linear coupling modes between the bar and spiral arms [37]. The leading ends of the bar are important for modelling the long bar observations.

3 The long bar-boxy bulge. Quantitative analysis.

In [27], we applied a similar technique as that used by observers to analyse the boxy bulge [42, 3] and the long bar in the MW [4, 9, 8, 10]. This technique consists in identifying the maxima of the magnitude distribution of red clump stars along various line-of-sight (l and b correspond to longitude and latitude, respectively). Given the distribution of model particles with distance modulus (see Fig. 2; left panel) we fitted a Gaussian to the first peak. For comparison and clarification we show four histograms. Near the ends of the bar (see Fig. 2; left panel, plot *a*), we can identify in the histogram three main peaks, one corresponding to

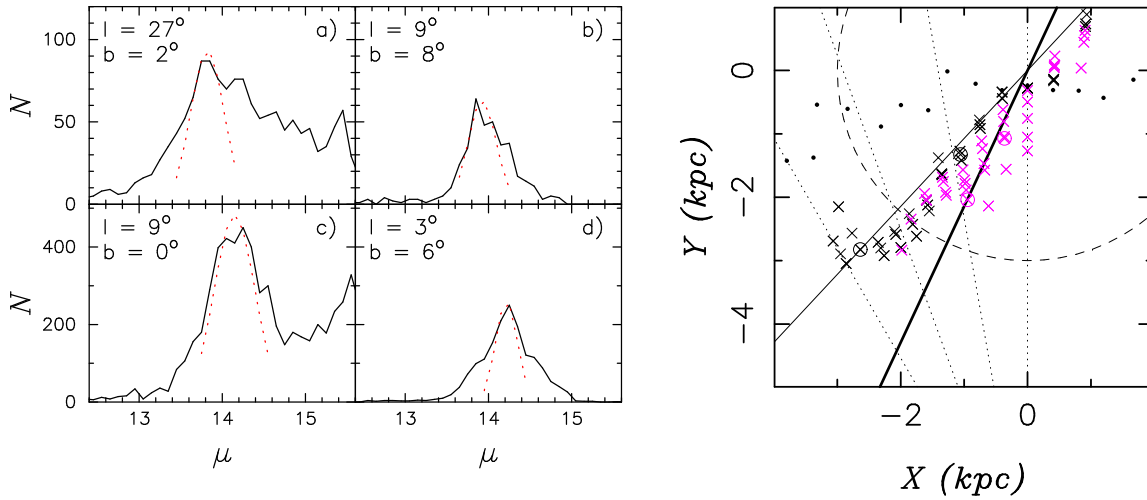


Figure 2: *Left panel:* Plots showing the distribution of particles with distance modulus in four fields as seen by an observer at the Sun’s position 8 kpc from the centre (from [27]). Plots a), c) show distributions in/near the Galactic plane in cones centred on the given longitude and latitude. Plots b), d) show histograms for cones through the boxy bulge. *Right panel:* Maxima of particle distributions versus distance modulus, for all fields in the disk plane (black crosses) and in the boxy bulge ($4^\circ \leq |b| \leq 8^\circ$, red crosses). The circled crosses correspond to the histograms shown on the left panel. The thick solid line shows the true orientation of the model, $\alpha = 25^\circ$. The thin line follows $\alpha' = 43^\circ$. In order to increase the signal the simulation has been symmetrized vertically.

the flat end of the bar, one to the spiral arm on the back and one corresponding to the end of the disk. The second histogram shows the distribution of stars when looking at a field well above the plane, but in the region of the thick structure (the boxy-bulge). The third histogram shows a field at the same longitude as the previous one but when looking through the plane. The fourth histogram shows a field close to the centre of the model. The maxima of the histograms together with those for other fields are projected on the MW plane in Fig. 2 (right panel). We can see how there are two sets of points, those in the plane following the line of $\sim 43^\circ$ and the other group, following the line at $\sim 25^\circ$.

The maxima of the line-of-sight distance distributions in the Galactic plane occur at distances somewhat further than the maxima of the line-of-sight density distributions, due to the volume effect in the star counts. This effect is stronger in the galactic plane (Fig. 2; right panel). Assuming a plausible orientation ($\alpha = 25^\circ$), this explains part of the observational signature which was previously used to infer the existence of a second long bar. If in addition we choose a model snapshot where the bar has leading ends, as seen in Fig. 1, most of the long bar signature in the star count data can be reproduced. While not made specially to fit to the MW, this model thus illustrates that the traditional Galactic bar (the boxy bulge) and the more recently inferred long bar can plausibly be explained by a single *boxy bulge/bar* structure (more details in [27]).

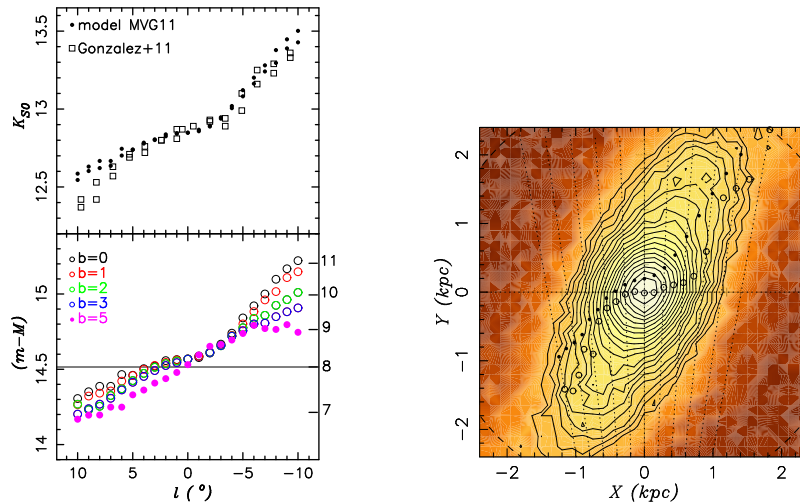


Figure 3: *Left panel*: Maxima of observed and model magnitude distributions for red clump (RC) giant stars in bulge fields as a function of longitude. Top: Simulated RC maxima for strips with latitudes $[b = 1 \pm 0.5^\circ]$ and $[0 \pm 0.5^\circ]$ (black dots), compared with data from the VVV survey at $b = \pm 1^\circ$ ([19], open squares). Bottom: RC maxima in strips with different latitudes. The change of slope around $|l| = 4^\circ$ seen at low latitudes is absent at $b = 5^\circ$. The horizontal line illustrates the assumed distance to the GC. *Right panel*: Face-on surface density of the particles with $|z| < 300$ pc, with overplotted maxima of the line-of-sight density distributions (open circles) and maxima of the simulated line-of-sight RC magnitude distributions (full circles) for particles in the latitude range $|b| \leq 2^\circ$. (From [18])

4 The inner region of our Galaxy.

The inner region of the MW has been studied by analysing the red clump (RC) star counts. Nishiyama et al. (2005, [32]) determined the maximum of the RC magnitude distribution for different pencil beams at various longitudes at $b = -1^\circ$. They found a clear change of slope in the RC longitude profile at $l \sim 5^\circ$, finding a steep slope in the outer bulge and a flatter slope in the nuclear regions. Recently, Gonzalez et al. (2011, [19]) analysed new RC star counts from the VVV survey and found excellent agreement with Nishiyama et al. This flattening has been interpreted as a distinct structure in the inner galactic bulge, and very often associated to a nuclear/secondary bar in the MW [1]. Taking the model presented in this work, we compute the smooth histograms of distance modulus for the different beams in a similar way as in Fig. 2 (left panel). We then take the maximum of each histogram. We use $M_K = -1.72$ to shift the model distance moduli to the magnitude scale of the data and plot it against the observed data. As we can see in Fig. 3 the model used in [18] reproduced the flattening of the longitudinal profile. But the simulated model bulge does not contain such a structure. The flattening of the profile corresponds to the almost axisymmetric region in the inner parts of the model (Fig. 3; left panel).

Recently, the longitudinal profile of our model for $b = -3^\circ$ has been compared with VVV data obtaining an extremely good agreement [20]. When comparing our model with the OGLE data [31] there is an excellent agreement among their profiles for $b = 3^\circ$ and $b = 5^\circ$ and those from our model, in particular regarding the slope.

5 Comparison between observational kinematical data and the proposed model

Up to now we have presented a model for the MW bar and bulge which has been formed through secular evolution. This type of bar/boxy bulges present in general cylindrical rotation. So our next step is to compare this model with kinematic data from recent spectroscopic surveys such as BRAVA [23]. We use a modified version of the NMAGIC code [13] to study the properties of the MW bar. By changing the contribution of the particles in each of the fields (BRAVA fields) we modify our original model to match the kinematical data. We explore different parameters to obtain the minimum χ^2 obtaining an upper limit for the pattern speed of ~ 42 km/sec/kpc and an orientation angle of $\alpha = 25^\circ$. See Fig. 4 for a comparison of one of our best models with BRAVA data [28].

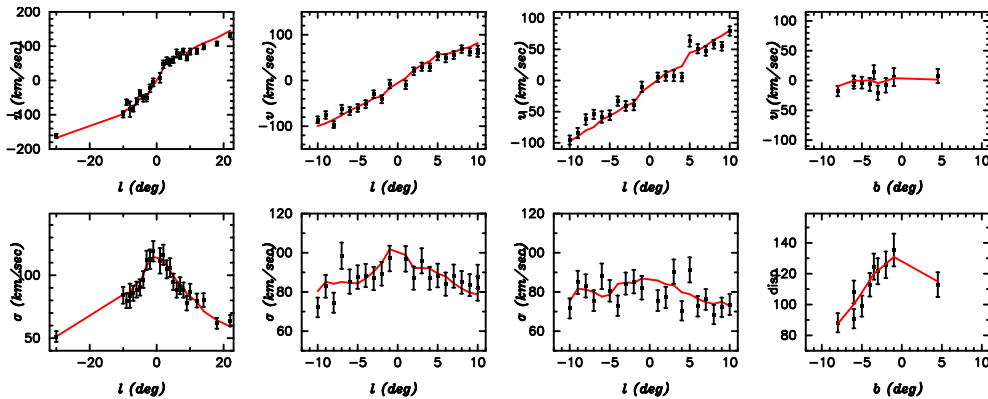


Figure 4: One of our best dynamical models (line) for the galactic bulge-bar of the MW compared to BRAVA data (points). From left to right: mean velocities (top) and velocity dispersions (bottom) in fields at latitudes $b = -4^\circ, -6^\circ, -8^\circ$ with longitude, and along the minor axis with latitude.

6 Summary

In this work we present a new structure for the inner parts ($r \leq 5$ kpc) of the MW. The new properties of the galactic bar are: the length of the bar of $r_b = 4.5$ kpc, the orientation angle $\alpha = 25^\circ$, and the pattern speed of $\Omega_b \leq 42$ km/sec/kpc. This new bar is formed by bar instability, buckling instability and secular evolution of a purely exponential disk embedded in a live dark matter halo.

We find of extreme importance for the interpretation and better understanding of the future upcoming galactic surveys (GAIA, ESO-GAIA, HERMES, APOGEE, etc.) to revisit previous works based on the dynamical effects of the galactic bar. Among the results that could be affected by these new feature are those highly affected by resonances, such as moving groups, lv -diagrams, number and position of the spiral arms, rings in the disk and radial mixing due to resonances.

Acknowledgements

I am thankful to the organizers of this session for inviting me. This work would not have been possible without Ortwin Gerhard and the Dynamics Group at MPE.

References

- [1] Alard, C. 2001, *A&A*, 379, L44
- [2] Athanassoula, E. 2006, arXiv:astro-ph/0610113
- [3] Babusiaux, C., Gilmore, G., & Irwin, M., 2005, *MNRAS*, 359, 985
- [4] Benjamin, R. A., Churchwell, E., Babler, B. L., & Indebetouw, R. 2005, *ApJ*, 630, L149
- [5] Binney J., Gerhard, O., & Spergel, D. 1997, *MNRAS*, 288, 365
- [6] Bissantz, N., Debattista, V. P., & Gerhard, O. 2004, *ApJ*, 601, L155
- [7] Bureau, M. & Freeman, K. C. 1999, *AJ*, 118, 126
- [8] Cabrera-Lavers, A., González-Fernández, C., Garzón, F., et al. 2008, *A&A*, 491, 781
- [9] Cabrera-Lavers, A., Hammersley, P. L., González-Fernández, C., et al. 2007, *A&A*, 465, 825
- [10] Churchwell, E., Babler, B.L., Meade, M.R., et al. 2009, *PASP*, 121, 213
- [11] Combes, F., Debbasch, F., Friedli, D., & Pfenniger, D., 1990, *A&A*, 233, 82
- [12] Combes, F. & Sanders, R. H. 1981, *A&A*, 96, 164
- [13] de Lorenzi, F., Debattista, V. P., Gerhard, O., & Sambhus, N. 2007, *MNRAS*, 376, 71
- [14] de Vaucouleurs, G. 1964, in *Proceedings of IAU Symp. 20*, F. J. Kerr (ed.), p. 195
- [15] Dubinski, J., Berentzen, I., & Shlosman, I. 2009, *ApJ*, 697, 293
- [16] Dwek, E., Arendt, R. G., Hauser, M. G., et al. 1995, *ApJ*, 445, 716
- [17] Fux, R. 1997, *A&A*, 327, 983
- [18] Gerhard, O. & Martinez-Valpuesta, I. 2012, *ApJ*, 744, L8
- [19] Gonzalez, O. A., Rejkuba, M., Minniti, D., et al. 2011, *A&A*, 534, L14
- [20] González, O. A., Rejkuba, M., Zoccali, M., et al. 2012, *A&A*, 543, A13
- [21] Hammersley, P. L., Garzón, F., Mahoney, T. J., et al. 2000, *MNRAS*, 317, L45
- [22] Heller, C. H. & Shlosman, I. 1994, *ApJ*, 424, 84

- [23] Kunder, A., Koch, A., Rich, R. M., et al. 2012, *AJ*, 143, 57
- [24] López-Corredoira, M., Cabrera-Lavers, A., & Gerhard, O. E. 2005, *A&A*, 439, 107
- [25] López-Corredoira, M., Cabrera-Lavers, A., Mahoney, T. J., et al. 2007, *AJ*, 133, 154
- [26] Martinez-Valpuesta, I., Shlosman, I., & Heller, C. 2006, *ApJ*, 637, 214
- [27] Martinez-Valpuesta, I. & Gerhard O. 2011, *ApJ*, 734, L20
- [28] Martinez-Valpuesta, I. & Gerhard, O. 2013, *ApJ*, 766, 3
- [29] Merrifield, M. R. & Kuijken, K., 1999, *A&A*, 345, L47
- [30] Ness, M. & Freeman, K. 2012, in *European Physical Journal Web of Conferences* 19, p. 6003
- [31] Nataf, D. M., Gould, A., Fouqué, P., et al. 2012, arXiv:1208.1263
- [32] Nishiyama, S., Nagata, T., Baba, D., et al. 2005, *ApJ*, 621, L105
- [33] Raha, N., Sellwood, J. A., James, R. A., & Kahn, F. D. 1991, *Nature*, 352, 411
- [34] Rattenbury, N. J., Mao, S., Debattista, V. P., et al. 2007, *MNRAS*, 378, 1165
- [35] Rattenbury, N. J., Mao, S., Sumi, T., & Smith, M. C. 2007, *MNRAS*, 378, 1064
- [36] Rautiainen, P. & Salo, H. 2000, *A&A*, 362, 465
- [37] Tagger, M., Sygnet, J. F., Athanassoula, E., & Pellat, R. 1987, *ApJ*, 318, L43
- [38] Romero-Gómez, M., Athanassoula, E., Antoja, T., & Figueras, F. 2011, *MNRAS*, 418, 1176
- [39] Shen, J., Rich, R. M., Kormendy, J., et al. 2010, *ApJ*, 720, L72
- [40] Stanek, K. Z. 1995, *ApJ*, 441, L29
- [41] Stanek, K. Z., Mateo, M., Udalski, A., et al. 1994, *ApJ*, 429, L73
- [42] Stanek, K. Z., Udalski, A., Szymanski, M., et al. 1997, *ApJ*, 477, 163
- [43] Sumi, T., Wu, X., Udalski, A., et al. 2004, *MNRAS*, 348, 1439
- [44] Weiland, J. L., Arendt, R. G., Berriman, G. B., Dwek, E., et al. 1994, *ApJ*, 425, L81